IET Communications

Research Article

IET Journals
The Institution of Engineering and Technology

ISSN 1751-8628
Received on 17th March 2019
Revised 30th May 2019
Accepted on 23rd August 2019
doi: 10.1049/iet-com.2019.0295
www.ietdl.org

M-ary code-shifted differential chaos shift keying with in-phase and quadrature code index modulation

Xiangming Cai[1], Weikai Xu[1] ✉, Lin Wang[1], Fang Xu[1]

[1]*School of Information Science and Engineering, Xiamen University, Xiamen 361005, People's Republic of China*

✉ *E-mail: xweikai@xmu.edu.cn*

Abstract: In this study, an *M*-ary code-shifted differential chaos shift keying system with in-phase and quadrature code index modulation (I/Q-CIM-CS-MDCSK) is presented. In the proposed system, the information bits are conveyed not only by the *M*-ary constellation symbols, but also by the specific Walsh codes indices corresponding to the in-phase and quadrature branches of *M*-ary information bearing signals. Since the reference signal and the multiple *M*-ary information bearing signals are overlapped and transmitted within the identical time slot in a parallel manner, the spectral efficiency of the I/Q-CIM-CS-MDCSK system is enhanced significantly. In addition, the analytical bit error rate (BER) expressions for the presented system are derived under the additive white Gaussian noise and multipath Rayleigh fading channels. Finally, the BER performance of the proposed system is compared to other chaotic communication systems. The results manifest that the I/Q-CIM-CS-MDCSK system is a promising and competitive chaotic communication scheme.

1 Introduction

The excellent properties of chaotic signals, such as wideband, good correlation and high robustness to multipath degradation [1, 2] and superior communication security [3], have made them a perfect candidate for spread spectrum (SS) communications [4–8]. As we well-known, differential chaos shift keying (DCSK) [9] is the most popular non-coherent chaotic modulation scheme, because the complex chaotic synchronisation and the channel state information are not necessary for DCSK system. In DCSK scheme, each bit duration is partitioned into two equal time slots, where the first time slot is used to carry the reference signal and the following second time slot is provided for the information bearing signal. Accordingly, DCSK scheme inherently suffers from low data rate which is due to the fact that half of the bit duration is used for transmitting non-information-bearing reference samples [10].

Since the explosion of data services have witnessed the societal changes, the growing appetite for high data rate accelerates the development of wireless communication system. In this vein, the conventional DCSK scheme may be not suitable for the current requirement of high data rate, which urges the research buddies to design the meritorious high-data-rate chaotic communication systems. In [11], quadrature chaos shift keying (QCSK) is characterised by the alike bandwidth and similar BER performance as compared to DCSK system, but it doubles the data rate. Based on this work, some researches extend the QCSK scheme into its *M*-ary version, namely *M*-ary DCSK [12], which can offer higher data rate. Although the *M*-ary DCSK system can elevate the data rate to a great extent by adjusting the modulation order, this improvement is apparently at the expend of BER performance loss. Explicitly, this phenomenon can be explained by the fact that when the modulation order is enlarged, the Euclidean distance between adjacent constellation points is shrunk causing the poor BER performance. Therefore, there is a trade-off between the data rate and BER performance.

Benefiting from the perfect orthogonality of disparate Walsh code sequences, the authors of [13] make a powerful combination between the Walsh code and the conventional DCSK system, and then a new non-coherent code-shifted DCSK (CS-DCSK) system is presented. In CS-DCSK system, not only is the delay line in the receiver terminal well solved, but the spectral efficiency is enhanced because the reference and information signals are overlapped and transmitted in the same time slot. Subsequently, the CS-DCSK system is extended to generalised CS-DCSK (GCS-DCSK) [14] by the identical authors which supports the transmission of data streams in a parallel manner. Inspired by the above meritorious works, multilevel code shifted differential chaos shift keying (MCS-DCSK) [15] is reported to maximise the utilisation of Walsh code and improve the BER performance in contrast to GCS-DCSK system. In [16], a high-data-rate CS-DCSK scheme, namely HCS-DCSK, is presented in which the different chaotic codes, rather than the limited Walsh code sequences, are applied to separate the reference and information bearing signals. By integrating the Walsh code sequence with Hilbert transform to construct the orthogonal basis sets, orthogonal multilevel DCSK (OM-DCSK) is reported in [17] to achieve the high data rate, high energy efficiency, better data security and BER performance. More recently, by using the orthogonal Walsh code sequences to bear the in-phase and quadrature components of *M*-ary constellation symbol, the authors of [18] propose a new MCS-DCSK with *M*-ary modulation. In this configuration, the spectral efficiency, data rate and BER performance are improved significantly compared to its rivals.

In the past few years, a promising modulation technique called code index modulation (CIM) [19, 20] has been developed arming to increase the data rate and reduce energy consumption while being sample to implement. Based on this initial work, CIM has triggered rapid advances in the field of chaotic communications [21, 22]. The use of the Walsh code index as an additional information-bearing unit increases the data rate and spectral efficiency. For example, code-shifted DCSK with index modulation (CIM-CS-DCSK) [21] can carry both modulated bits and mapped bits within single CIM-CS-DCSK symbol which makes a contribution in the aspect of improving data rate. More recently, by combining the short reference DCSK [23] with the promising CIM technique, the authors of [22] proposed a new chaotic modulation scheme namely CIM-DCSK, where two performance optimisation algorithms are applied to improve its BER performance effectively. In addition, with the benefits of index modulation (IM), a non-coherent commutation code index DCSK system, referred to as CCI-DCSK, was presented in [24] with the target of obtaining high data rate and spectral efficiency. Since the different permutations are exploited, permutation index DCSK (PI-DCSK) [25] scheme not only boosts the data rate, but also improves the security of transmitted data. In [26], a non-coherent DCSK with dual-IM (DCSK-DIM) was proposed to improve BER performance with high hardware complexity, and its

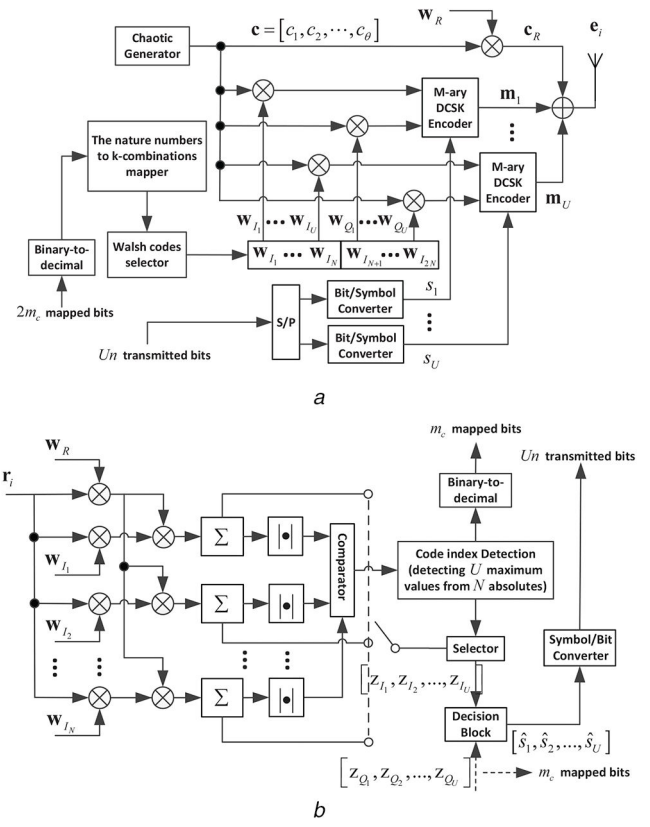

Fig. 1 *Block diagram of the I/Q-CIM-CS-MDCSK system*
(a) Transmitter, ***(b)*** Receiver

BER performance improvement is also at the expense of low spectral efficiency because lots of time slot resources are required.

Motivations and contributions: Inspired by the meritorious researches of [12, 18, 21, 27], we propose an M-ary code-shifted differential chaos shift keying scheme with in-phase/quadrature CIM in this paper. Differed from the construction of the conventional M-ary DCSK [12], the orthogonal Walsh code sequences corresponding to in-phase and quadrature branches are applied to carry the M-ary constellation symbol. Unlike the recently proposed CIM-CS-DCSK system [21], we extend the index domain to include in-phase and quadrature dimensions in I/Q-CIM-CS-MDCSK system, which means two different indices are used and better BER performance turns available. In this configuration, the system complexity is further reduced, because there is no demand of the complex Hilbert filter which is necessary for conventional M-ary DCSK. Due to the benefit of in-phase and quadrature CIM and the new-designed M-ary DCSK, apparently, we can make a combination of the new-designed M-ary DCSK [27] and the in-phase and quadrature CIM for the purpose of high data rate, high energy efficiency, low complexity and excellent BER performance, which is desirable for the case of low-cost, low-power and low-complexity applications.

The rest of this paper is organised as follows. The Section 2 presents the system model of I/Q-CIM-CS-MDCSK. Then, the performance analysis of the proposed system is given in Section 3. The numerical results are provided in Section 4. Finally, some conclusions are found in Section 5.

2 System model

2.1 Transmitter

The system model for I/Q-CIM-CS-MDCSK is presented in Fig. 1. Clearly, $2m_c + Un$ bits are transmitted in single I/Q-CIM-CS-MDCSK symbol, where the $2m_c$ bits are provided for mapped bits and the Un bits are used for transmitting the modulated bits. Besides, the total mapped bits are composed of the mapped bits of in-phase component and quadrature component, respectively, where both of them is equal to m_c. Then, U denotes the number of M-ary information bearing signals and each M-ary information bearing signal can carry $n = \log_2 M$ bits, where M denotes the modulation order of the M-ary DCSK encoder. At the transmitter, the chaotic generator generates a θ-length chaotic signal $\boldsymbol{x} = [x_1, x_2, \ldots, x_\theta]$, then we use Walsh codes to extend the chaotic signal $\boldsymbol{x}$. Therefore, the reference signal $\boldsymbol{c}_R$ can be expressed as $\boldsymbol{c}_R = \boldsymbol{w}_R \otimes \boldsymbol{x}$, where $\boldsymbol{w}_R = [w_{R,1}, w_{R,2}, \ldots, w_{R,P}]$ is Walsh code sequence with length P and $\otimes$ denotes Kronecker product. In addition, the uth M-ary information bearing signal can be represented in the vector form as $\boldsymbol{m}_u = a_u \boldsymbol{w}_{I_u} \otimes \boldsymbol{x} + b_u \boldsymbol{w}_{Q_u} \otimes \boldsymbol{x}$, where a_u and b_u represent the real and imaginary parts for the uth M-ary constellation symbol s_u. $\boldsymbol{w}_{I_u} = [w_{I_u,1}, w_{I_u,2}, \ldots, w_{I_u,P}]$ is a Walsh code with the code index $\{I_u\}_{u=1}^{U}$ chosen from a code set $\{\boldsymbol{w}_{I_u}\}_{u=1}^{N}$ including N Walsh codes, where $N = \frac{P}{4}$. Similar, $\boldsymbol{w}_{Q_u} = [w_{Q_u,1}, w_{Q_u,2}, \ldots, w_{Q_u,P}]$ is another Walsh code with code index $\{Q_u\}_{u=1}^{U}$ chosen from a code set $\{\boldsymbol{w}_{Q_u}\}_{u=N+1}^{2N}$ including N Walsh codes. It should be noted that the in-phase code index $\{I_u\}_{u=1}^{U}$ and quadrature code index $\{Q_u\}_{u=1}^{U}$ are determined by different in-phase and quadrature mapped bits, respectively. Hence, the baseband discrete I/Q-CIM-CS-MDCSK symbol can be stated as

$$\boldsymbol{e}_i = \boldsymbol{w}_R \otimes \boldsymbol{x} + \sum_{u=1}^{U} \left(a_u \boldsymbol{w}_{I_u} \otimes \boldsymbol{x} + b_u \boldsymbol{w}_{Q_u} \otimes \boldsymbol{x}\right), \tag{1}$$

where logistic map $x_{j+1} = 1 - 2x_j^2$, $j = 0, 1, \ldots$, is used to generate the chaotic signal in this paper. The spreading factor of this system is defined as $\beta = P\theta$. In this paper, The selected in-phase and quadrature code indices are obtained by the natural numbers to k-combinations mapping method [21]. Therefore, the number of mapped bits corresponding to the in-phase component can be calculated as

$$m_c = \left\lfloor \log_2 \left[\binom{N}{U} \right] \right\rfloor,$$

where

$$\binom{N}{U} = \frac{N!}{U!(N-U)!}$$

is the combination number and $\lfloor \cdot \rfloor$ denotes the floor function.

2.2 Receiver

In this paper, a well studied channel model [12, 28, 29] with Rayleigh distributed channel coefficients is considered. The Rayleigh probability density function of the channel coefficient α is written as $f_\alpha(z) = (z/\chi^2)\exp\left(-(z^2/2\chi^2)\right)$, where $\chi > 0$ is the scale parameter of the distribution. When the signal in the transmitter terminal passes through the Rayleigh fading channel with additive white Gaussian noise (AWGN), the received signal is represented in a vector form as

$$\boldsymbol{r}_i = \sum_{l=1}^{L} \alpha_{i,l} \boldsymbol{e}_{i-\tau_{i,l}} + \boldsymbol{n}_i, \tag{2}$$

where $\alpha_{i,l}$ is the channel coefficient and $\tau_{i,l}$ denotes the time delay corresponding to lth path. L is the number of the paths. Besides, $\boldsymbol{n}_i$ denotes the AWGN with zero mean and covariance $\frac{N_0}{2}\boldsymbol{I}$, where $\boldsymbol{I}$ is the identity matrix. When the channel parameters $L = 1$, $\alpha_{i,1} = 1$ and $\tau_{i,1} = 0$ are satisfied, this channel becomes the ordinary AWGN channel.

As shown in Fig. 1*b*, since the in-phase branch is similar to quadrature branch at the receiver terminal, we only consider the case of in-phase branch in the following analysis and the analysis of quadrature branch can be obtained in an alike manner. Besides, the subscript i will be omitted for simplicity. According to the

block diagram of I/Q-CIM-CS-MDCSK receiver, the output of the u^{th} in-phase branch can be obtained as

$$z_{I_u} = [\boldsymbol{r} \odot (\boldsymbol{w}_R \otimes \mathbf{1}_{1\times\theta})][\boldsymbol{r} \odot (\boldsymbol{w}_{I_u} \otimes \mathbf{1}_{1\times\theta})]^{\mathrm{T}}, \quad u = 1, 2, \ldots, N, \tag{3}$$

where $\odot$ denotes the Hadamard product operation and $[\cdot]^{\mathrm{T}}$ represents the transposition operation. Additionally, $\mathbf{1}_{1\times\theta} = [1, 1, \ldots, 1]$ denotes a unit vector with length θ. In particular, let $|\boldsymbol{z}_I| = \{|z_{I_1}|, |z_{I_2}|, \ldots, |z_{I_N}|\}$, thus we can get U indices $\{I_u\}_{u=1}^{U}$ by selecting the U maximums from the set $|\boldsymbol{z}_I|$ via the code indices estimation algorithm [21]. Then, we use set $|\boldsymbol{z}'_I|$ to represent the selected U maximums, i.e. $|\boldsymbol{z}'_I| = \{|z'_{I_1}|, |z'_{I_2}|, \ldots, |z'_{I_U}|\}$. Similarly, according to the above method, $|\boldsymbol{z}_Q|$, $\{Q_u\}_{u=1}^{U}$ and $|\boldsymbol{z}'_Q|$ for the quadrature branch can be obtained. Denote $z'_u = z'_{I_u} + \sqrt{-1}z'_{Q_u}$. Hence, the M-ary constellation symbols corresponding to the above U indices can be estimated by the minimum distance decision criterion, namely

$$\hat{s}_u = \arg\min_{s\in S}\left(|z'_u - s|^2\right), \quad u = 1, 2, \ldots, U, \tag{4}$$

where set S contains all possible M-ary constellation points. Finally, the mapped bits can be retrieved via converting the selected indices from the decimal number to a binary number, while the modulated bits can be recovered by the symbol-to-bit converter.

3 Performance analysis

As stated earlier, the total transmitted bits within single I/Q-CIM-CS-MDCSK symbol is composed of $2m_c$ mapped bits and Un modulated bits. Therefore, the total bit error rate of I/Q-CIM-CS-MDCSK system is the function of mapped bits and modulated bits, described as

$$P_T = \frac{2m_c}{2m_c + Un}P_{\mathrm{map}} + \frac{Un}{2m_c + Un}P_{\mathrm{mod}}, \tag{5}$$

where P_{map} is the bit error probability of mapped bits and P_{mod} is the BER of modulated bits. According to [24, 25], the error probabilities P_{map} and P_{mod} can be given as

$$P_{\mathrm{map}} = \frac{2^{(m_c-1)}}{2^{m_c}-1}P_{\mathrm{ed}}, \tag{6}$$

$$P_{\mathrm{mod}} = P_{\mathrm{e}}(1 - P_{\mathrm{ed}}) + \frac{1}{2}P_{\mathrm{ed}}, \tag{7}$$

where P_{ed} and P_{e} denote the average erroneous Walsh code detection probability and the BER of modulated bits with correct Walsh code detection, respectively. According to the Appendix, when the Walsh code detection for the in-phase branch is correct, we can rewrite the mean and variance of decision variable z_{I_u} described as

$$\mu_{I,1} = \sum_{l=1}^{L}\alpha_l^2\frac{2a_uE_s}{1+U}, \tag{8}$$

$$\sigma_{I,1}^2 = 2\sum_{l=1}^{L}\alpha_l^2E_sN_0 + \beta\frac{N_0^2}{2}. \tag{9}$$

Similarly, in quadrature branch, the mean and variance of z_{Q_u} can be obtained as

$$\mu_{Q,1} = \sum_{l=1}^{L}\alpha_l^2\frac{2b_uE_s}{1+U}, \tag{10}$$

$$\sigma_{Q,1}^2 = 2\sum_{l=1}^{L}\alpha_l^2E_sN_0 + \beta\frac{N_0^2}{2}. \tag{11}$$

According to [12], we can be aware of that the decision variables z_{I_u} and z_{Q_u} are independent Gaussian variables with the means $\mu_{I,1} = \sum_{l=1}^{L}\alpha_l^2(2a_uE_s/(1+U))$ and $\mu_{Q,1} = \sum_{l=1}^{L}\alpha_l^2(2b_uE_s/(1+U))$, respectively. Moreover, both decision variables have the identical variance $\sigma^2 = \sigma_{I,1}^2 = \sigma_{Q,1}^2 = 2\sum_{l=1}^{L}\alpha_l^2E_sN_0 + \beta(N_0^2/2)$. Thus, the error probability P_{e} for the modulated bits is given as [12, 18]

$$P_{\mathrm{e}} \simeq \frac{2}{\log_2 M}\int_{\frac{\pi}{M}}^{\pi}\left[\frac{1}{2\pi}\exp\left(-\frac{\rho^2}{8}\right) + \exp\left(-\frac{\rho^2\sin^2\varphi}{8}\right) \times \frac{\rho\cos\varphi}{2\sqrt{2\pi}}Q\left(-\frac{\rho\cos\varphi}{2}\right)\right]\mathrm{d}\varphi \tag{12}$$

where

$$\rho = \frac{8\gamma_s}{(1+U)\sqrt{8\gamma_s + 2\beta}}, \tag{13}$$

$$Q(x) = \frac{1}{\sqrt{2\pi}}\int_x^{+\infty}\exp\left(-\frac{t^2}{2}\right)\mathrm{d}t, \tag{14}$$

then $\gamma_s = \sum_{l=1}^{L}\alpha_l^2\frac{E_s}{N_0}$ is the symbol signal-to-noise ratio (SNR).

Since the Walsh code detection for in-phase branch is similar to that of quadrature branch, we only analyse the erroneous Walsh code detection probability of in-phase branch for simplification. As observed in the Appendix, the decision variables z_{I_u} and $\hat{z}_{I_u}$ are independent Gaussian variables with the means $\mu_{I,1}$ and $\mu_{I,2}$, respectively, and with the same variances $\sigma^2 = \sigma_{I,1}^2 = \sigma_{I,2}^2$. Hence, the variables $|z_{I_u}|$ and $|\hat{z}_{I_u}|$ follow the folded normal distribution. According to [30], the probability density function (PDF) of $|z_{I_u}|$ and the cumulative distribution function (CDF) of $|\hat{z}_{I_u}|$ are formulated as

$$f_{|z_{I_u}|}(x) = \frac{1}{\sqrt{2\pi\sigma^2}}\left\{\mathrm{e}^{-\frac{(x-\mu_{I,1})^2}{2\sigma^2}} + \mathrm{e}^{-\frac{(x+\mu_{I,1})^2}{2\sigma^2}}\right\}, \tag{15}$$

$$F_{|\hat{z}_{I_u}|}(x) = \mathrm{erf}\left(\frac{x}{\sqrt{2\sigma^2}}\right), \tag{16}$$

where $\mathrm{erf}(x) = (2/\sqrt{\pi})\int_0^x\mathrm{e}^{-t^2}\mathrm{d}t$, $x \geq 0$ represents the well-known error function. As a consequence, the erroneous Walsh code detection probability of in-phase branch can be calculated as [21]

$$P_{\mathrm{ed}}^{\mathrm{I}} = \frac{U}{\sqrt{2\pi\sigma^2}}\int_0^{\infty}\left\{1 - \left[\mathrm{erf}\left(\frac{x}{\sqrt{2\sigma^2}}\right)\right]^{N-U}\right\} \times [1 - F^*(x)]^{U-1}\left\{\mathrm{e}^{-\frac{(x-\mu_{I,1})^2}{2\sigma^2}} + \mathrm{e}^{-\frac{(x+\mu_{I,1})^2}{2\sigma^2}}\right\}\mathrm{d}x, \tag{17}$$

where $F^*(x)$ is the CDF of $|z_{I_u}|$ described as

$$F^*(x) = \frac{1}{2}\left[\mathrm{erf}\left(\frac{x-\mu_{I,1}}{\sqrt{2\sigma^2}}\right) + \mathrm{erf}\left(\frac{x+\mu_{I,1}}{\sqrt{2\sigma^2}}\right)\right]. \tag{18}$$

Similarly, we can obtain the erroneous Walsh code detection of quadrature component $P_{\mathrm{ed}}^{\mathrm{Q}}$ by using the above analysis method. In this vein, the average erroneous Walsh code detection probability is equal to

$$P_{\mathrm{ed}} = \frac{P_{\mathrm{ed}}^{\mathrm{I}} + P_{\mathrm{ed}}^{\mathrm{Q}}}{2}. \tag{19}$$

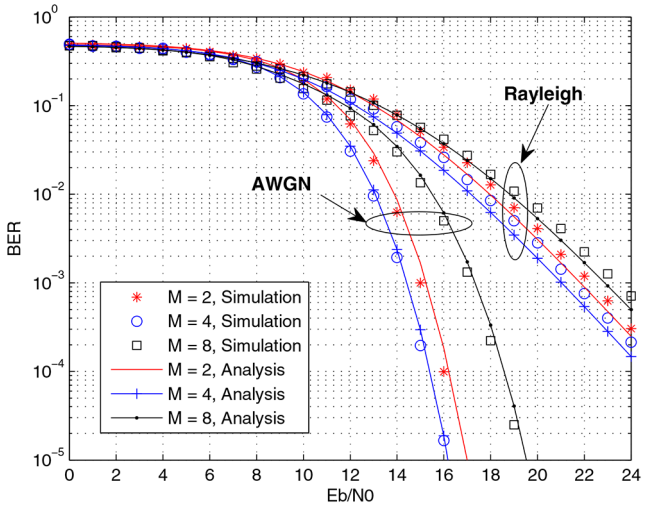

Fig. 2 *Performance of I/Q-CIM-CS-MDCSK system over AWGN and multipath Rayleigh fading channels with* $\beta = 512$, $P = 16$, $U = 1$ *and* $M = 2, 4, 8$

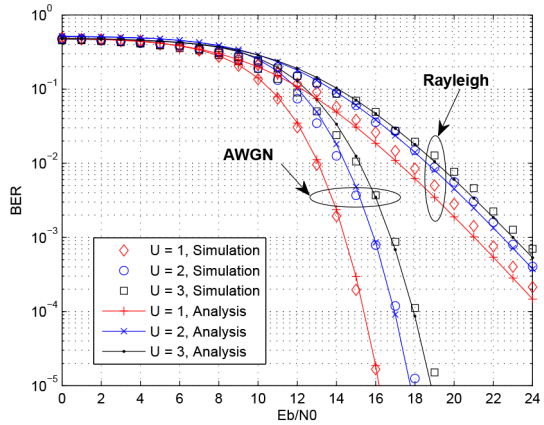

Fig. 3 *Effect of U on the performance of I/Q-CIM-CS-MDCSK system over AWGN and multipath Rayleigh fading channels with* $\beta = 512$, $P = 16$ *and* $M = 4$

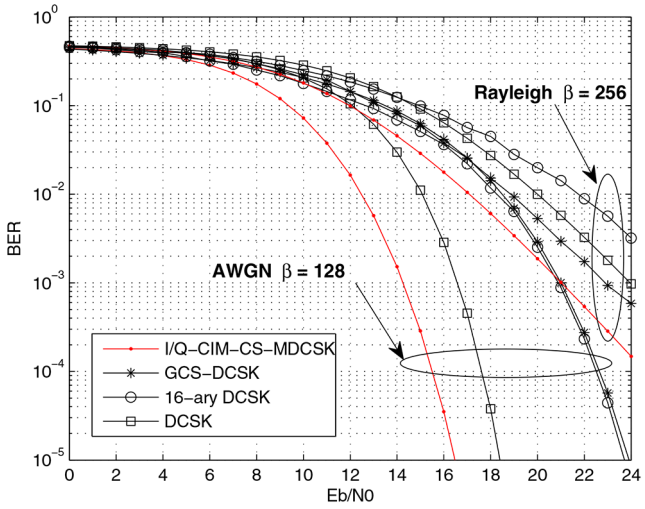

Fig. 4 *Performance comparison of I/Q-CIM-CS-MDCSK system and other chaotic modulation systems in AWGN and multipath Rayleigh fading channels, respectively*

To simplify the analysis, we only discuss L independent and identically-distributed (i.i.d) Raleigh-fading channel. Therefore, the probability density distribution of the symbol-SNR γ_s is given as [18, 28, 29]

$$f(\gamma_s) = \frac{\gamma_s^{L-1}}{(L-1)!\bar{\gamma}_c^{L}} \exp\left(-\frac{\gamma_s}{\bar{\gamma}_c}\right), \tag{20}$$

where $\bar{\gamma}_c$ denotes the average symbol-SNR per channel which can be defined as $\bar{\gamma}_c = (E_s/N_0)\mathrm{E}[\alpha_j^2] = (E_s/N_0)\mathrm{E}[\alpha_l^2]$, $j \neq l$ and $\sum_{l=1}^{L} \mathrm{E}[\alpha_l^2] = 1$. Finally, in the environment of multipath Rayleigh fading channel, the average bit error probability of the proposed I/Q-CIM-CS-MDCSK system is expressed as

$$\bar{P}_T = \int_0^{\infty} P_T \cdot f(\gamma_s)\, \mathrm{d}\gamma_s . \tag{21}$$

4 Numerical results and discussions

In this section, the BER performance of the I/Q-CIM-CS-MDCSK system is evaluated under AWGN and multipath Rayleigh fading channels. With respect to the multipath Rayleigh fading channel, a three-path channel is used with the same average gains, namely $\mathrm{E}[\alpha_1^2] = \mathrm{E}[\alpha_2^2] = \mathrm{E}[\alpha_3^2] = \frac{1}{3}$. then the time delays are uniformly distributed in the range of 0 and $2T_c$, where T_c denotes the chip duration.

As depicted in Fig. 2, the performance of the proposed system is shown under AWGN and multipath Rayleigh fading channels, where the modulation order is 2, 4 and 8, respectively. Clearly, the simulation results are in agreement with the theoretical results. Moreover, when $M = 4$, the proposed I/Q-CIM-CS-MDCSK system achieves the best BER performance. Except for the special case above, with the increasing of M, the BER performance of I/Q-CIM-CS-MDCSK system gradually worsens. This phenomenon arises from the fact that when the modulation order increases, the Euclidean distances of M-ary constellation symbols become smaller, which degrades the BER performance of the proposed I/Q-CIM-CS-MDCSK system.

In Fig. 3, we investigate the effect of U on the BER performance of the I/Q-CIM-CS-MDCSK system in both AWGN and multipath Rayleigh fading channels. A good match between simulations and the corresponding theoretical results can be easily observed, and it further verifies our theoretical derivations. As illustrated in Fig. 3, the performance of I/Q-CIM-CS-MDCSK system is deteriorating when U increases. For example, in AWGN channel, the I/Q-CIM-CS-MDCSK will require about 19 dB to achieve 10^{-5} BER level when $U = 3$. By contrast, on the condition of $U = 1$, the required SNR needed to achieve the same BER performance reduces to 16 dB. In this vein, the performance difference between $U = 1$ and $U = 3$ is 3 dB. Similar phenomenon can be observed in the case of fading channel. From another perspective, when $U = 1$, the number of the transmitted bits per symbol is 6. However, the total number of the counterparts is 10 when $U = 3$. It means the proposed I/Q-CIM-CS-MDCSK system can sacrifice some BER performance to increase throughput of the system.

To confirm the contribution of the proposed I/Q-CIM-CS-MDCSK system in terms of BER performance, as depicted in Fig. 4, we compared the I/Q-CIM-CS-MDCSK, GCS-DCSK and 16-ary DCSK systems. Then as a benchmark, the BER performance of the conventional DCSK system is also drawn in Fig. 4. In all systems above (except for DCSK system), the number of bits per symbol is set to 4. The order of Walsh code $P = 8$ is used for I/Q-CIM-CS-MDCSK and GCS-DCSK systems. Additionally, the modulation order of I/Q-CIM-CS-MDCSK is equal to 4. As shown in Fig. 4, the performance gain of the proposed I/Q-CIM-CS-MDCSK system over DCSK is about 2 dB in AWGN channel at BER level 10^{-5}, and greater gain can be obtained when we take GCS-DCSK and 16-ary DCSK systems into comparison. Explicitly, the performance improvement of I/Q-CIM-CS-MDCSK system is mainly owing to the fact that the in-phase and quadrature code IM promotes the proportion of mapped bits within the overall transmitted bits, and thus the required SNR needed to achieve a certain BER decreases.

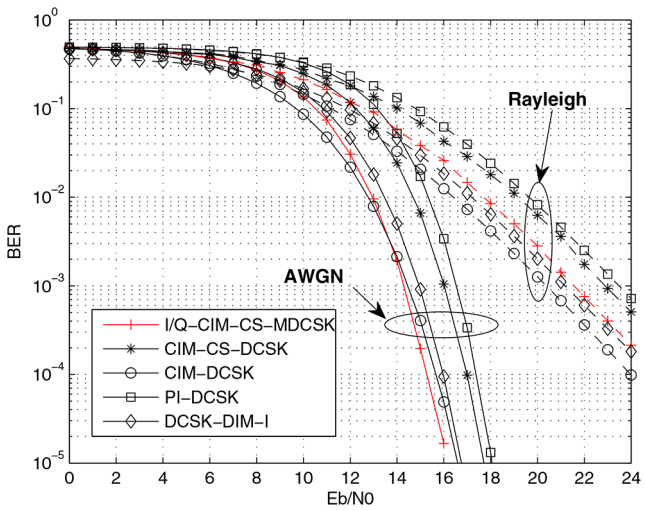

Fig. 5 *Performance comparison of the I/Q-CIM-CS-MDCSK system and other chaotic modulation systems with IM or code IM with* $\beta = 512$

As observed in Fig. 5, we make a BER performance comparison, over AWGN and multipath Rayleigh fading channels, between the I/Q-CIM-CS-MDCSK system and other chaotic modulation systems with IM or CIM, including CIM-CS-DCSK, CIM-DCSK, PI-DCSK and DCSK-DIM-I systems. Other significant simulation parameters are summarised as follows: $P = 16$, $U = 1$ and $M = 4$ are provided for I/Q-CIM-CS-MDCSK system. In CIM-CS-DCSK, the number of parallel data streams is 2 and the length of Walsh code sequence is equal to 8. As for PI-DCSK, the number of distinct permuted reference sequences is equal to 4. With regard to DCSK-DIM-I system, the number of time slots for information bearing signal is set to 2.

In AWGN channel, the proposed system achieves the best BER performance compared to its rivals in the high SNR region. In particular, I/Q-CIM-CS-MDCSK system has about 2 dB gain over PI-DCSK system at the BER level 10^{-5}. As expected, I/Q-CIM-CS-MDCSK can harvest almost 2 dB performance gain over CIM-CS-DCSK system which reveals that the proposed in-phase and quadrature CIM can make a larger contribution to CS-DCSK system and the M-ary modulation plays a significant role for I/Q-CIM-CS-MDCSK system as well in terms of BER performance. In multipath Rayleigh fading channel, although CIM-DCSK system outperforms the I/Q-CIM-CS-MDCSK system, the spectral efficiency of I/Q-CIM-CS-MDCSK system is better than that of CIM-DCSK system. It is due to the fact that the reference signal and information bearing signal are overlapping within the same time slot in I/Q-CIM-CS-MDCSK system, which results in the required spectrum resource is halved and thus the spectral efficiency is doubled. Although the BER performance of the proposed I/Q-CIM-CS-MDCSK system is slightly inferior to that of DCSK-DIM-I system over multipath Rayleigh fading channel, I/Q-CIM-CS-MDCSK system can achieve approximately 1 dB performance gain compared to DCSK-DIM-I system over AWGN channel. From another point of view, the BER performance improvement of DCSK-DIM-I system is at the expense of higher hardware complexity, because the Hilbert filter is necessary to accomplish dual-index modulation in DCSK-DIM-I system. In addition, since the DCSK-DIM-I system is based on time-slot index modulation, namely the positions of different active time slots are served as a new dimension for data transmission, lots of time slot resources are required in this system which leads to lower spectral efficiency. Therefore, the I/Q-CIM-CS-MDCSK system can achieve a satisfactory trade-off between the BER performance, hardware complexity and spectral efficiency with the appropriate parameters.

5 Conclusion

In this paper, an M-ary code-shifted differential chaos shift keying system with in-phase and quadrature code index modulation referred to as I/Q-CIM-CS-MDCSK is proposed. In the proposed system, since the reference signal and the multiple M-ary information signals are overlapped and transmitted within the identical time slot, I/Q-CIM-CS-MDCSK system can achieve superior spectral efficiency. Moreover, I/Q-CIM-CS-MDCSK system takes the advantages of in-phase and quadrature CIM as well as M-ary modulation techniques, which improves the data rate significantly and is conducive to BER performance improvement. To complete this research, we derive the analytical expressions of the proposed I/Q-CIM-CS-MDCSK system under AWGN and multipath Rayleigh fading channels, then the theoretical derivations are confirmed by our simulation results. Finally, the BER performance of I/Q-CIM-CS-MDCSK system and other chaotic modulation systems are compared. The obtained results of our analysis and discussion demonstrate the fact that the proposed system is promising and competitive in terms of its high data rate, high spectral efficiency, low complexity and satisfactory BER performance.

6 References

[1] Xia, Y., Tse, C.K., Lau, F.C.M.: 'Performance of differential chaos-shift-keying digital communication systems over a multipath fading channel with delay spread', *IEEE Trans. Circuits Syst. II*, 2004, **51**, (12), pp. 680–684

[2] Vali, R., Berber, S., Nguang, S.K.: 'Accurate derivation of chaos-based acquisition performance in a fading channel', *IEEE Trans. Wirel. Commun.*, 2012, **11**, (2), pp. 722–731

[3] Lynnyk, V., Čelikovský, S.: 'On the anti-synchronization detection for the generalized lorenz system and its applications to secure encryption', *Kybernetika*, 2010, **46**, (1), pp. 1–18

[4] Simon, M.K., Omura, J.K., Scholtz, R.A., *et al.*: '*Spread spectrum communications*' (Computer Science Press, Rockville, MD, USA, 1985)

[5] Heidari-Bateni, G., McGillem, C.: 'Chaotic sequences for spread spectrum: an alternative to pn-sequences'. Proc. IEEE Int. Conf. Selected Topics in Wireless Communications, Vancouver, BC, Canada, 1992, pp. 437–440

[6] Heidari-Bateni, G., McGillem, C.: 'A chaotic direct-sequence spread spectrum communication system', *IEEE Trans. Commun.*, 1994, **234**, (42), pp. 1524–1527

[7] Fang, Y., Han, G., Chen, P., *et al.*: 'A survey on dcsk-based communication systems and their application to UWB scenarios', *IEEE Commun. Surv. Tutor.*, 2016, **18**, (3), pp. 1804–1837

[8] Kaddoum, G.: 'Wireless chaos-based communication systems: a comprehensive survey', *IEEE Access*, 2016, **4**, pp. 2621–2648

[9] Kolumbán, G., Vizvari, G.K., Schwarz, W., *et al.*: 'Differential chaos shift keying: a robust coding for chaos communication'. Proc. Nonlinear Dynamics of Electronic Systems, Seville, Spain, 1996, pp. 92–97

[10] Lau, F.C.M., Tse, C.K.: '*Chaos-based digital communication systems*' (Springer, New York, NY, USA, 2003)

[11] Galias, Z., Maggio, G.M.: 'Quadrature chaos-shift keying: theory and performance analysis', *IEEE Trans. Circuits Syst. I*, 2001, **48**, (12), pp. 1510–1519

[12] Wang, L., Cai, G., Chen, G.: 'Design and performance analysis of a new multiresolution M-ary differential chaos shift keying communication system', *IEEE Trans. Wirel. Commun.*, 2015, **14**, (9), pp. 5197–5208

[13] Xu, W., Wang, L., Kolumbán, G.: 'A novel differential chaos shift keying modulation scheme', *Int. J. Bifur. Chaos*, 2011, **21**, (3), pp. 799–814

[14] Xu, W., Wang, L., Kolumbán, G.: 'A new data rate adaption communications scheme for code-shifted differential chaos shift keying modulation', *Int. J. Bifur. Chaos*, 2012, **22**, (8), pp. 1–8

[15] Huang, T., Wang, L., Xu, W., *et al.*: 'Multilevel code-shifted differential-chaos-shift-keying system', *IET Commun.*, 2016, **10**, (10), pp. 1189–1195

[16] Kaddoum, G., Gagnon, F.: 'Design of a high-data-rate differential chaos-shift keying system', *IEEE Trans. Circuits Syst. II*, 2012, **59**, (7), pp. 448–452

[17] Yang, H., Tang, W.K., Chen, G., *et al.*: 'System design and performance analysis of orthogonal multi-level differential chaos shift keying modulation scheme', *IEEE Trans. Circuits Syst. I*, 2016, **63**, (1), pp. 146–156

[18] Cai, X., Xu, W., Zhang, R., *et al.*: 'A multilevel code shifted differential chaos shift keying system with M-ary modulation', *IEEE Trans. Circuits Syst. II*, 2019, **66**, (8), pp. 1451–1455

[19] Kaddoum, G., Ahmed, M.F.A., Nijsure, Y.: 'Code index modulation: A high data rate and energy efficient communication system', *IEEE Commun. Lett.*, 2015, **19**, (2), pp. 175–178

[20] Kaddoum, G., Nijsure, Y., Tran, H.: 'Generalized code index modulation technique for high-data-rate communication systems', *IEEE Trans. Veh. Technol.*, 2016, **65**, (9), pp. 7000–7009

[21] Xu, W., Huang, T., Wang, L.: 'Code-shifted differential chaos shift keying with code index modulation for high data rate transmission', *IEEE Trans. Commun.*, 2017, **65**, (10), pp. 4285–4294

[22] Xu, W., Tan, Y., Lau, F.C.M., *et al.*: 'Design and optimization of differential chaos shift keying scheme with code index modulation', *IEEE Trans. Commun.*, 2018, **66**, (5), pp. 1970–1980

[23] Kaddoum, G., Soujeri, E., Nijsure, Y.: 'Design of a short reference non-coherent chaos-based communication systems', *IEEE Trans. Commun.*, 2016, **64**, (2), pp. 680–689

[24] Herceg, M., Vranješ, D., Kaddoum, G., *et al.*: 'Commutation code index dcsk modulation technique for high-data-rate communication systems', *IEEE Trans. Circuits Syst. II*, 2018, **65**, (65), pp. 1954–1958

[25] Herceg, M., Vranješ, D., Kaddoum, G., *et al.*: 'Permutation index dcsk modulation technique for secure multiuser high-data-rate communication systems', *IEEE Trans. Veh. Technol.*, 2018, **67**, (4), pp. 2997–3011
[26] Cai, X., Xu, W., Wang, L., *et al.*: 'Design and performance analysis of differential chaos shift keying system with dual-index modulation', *IEEE Access*, 2019, **7**, pp. 26867–26880
[27] Tan, Y., Xu, W., Hu, W., *et al.*: 'Efficient and robust *M*-ary differential chaos shift keying scheme with code index modulation', *IET Commun.*, 2019, **13**, (2), pp. 232–242
[28] Kaddoum, G., Richardson, F., Gagnon, F.: 'Design and analysis of a multi-carrier differential chaos shift keying communication system', *IEEE Trans. Commun.*, 2013, **61**, (8), pp. 3281–3291
[29] Proakis, J.G., Salehi, M.: '*Digital communications*' (McGraw-Hill, New York, NY, USA, 2007)
[30] Papoulis, A.: '*Probability random variables and stochastic processes*' (McGraw-Hill, New York, NY, USA, 1991)

7 Appendix

According to (3), the decision variable z_{I_u} can be expressed in a detail form as (see (22)) .

Generally, the decision variable z_{I_u} corresponding to in-phase branch can be decomposed into three independent terms, namely A, B and C, respectively. When the in-phase Walsh code detection is correct, i.e. $n = I_u$, the component A_1 is given as follows:

(see (23))

Then, B_1 and C_1 can be written as

$$B_1 = \sum_{p=1}^{P}\sum_{j=1}^{\theta} w_{R,p} w_{I_u,p} \left[n_{(p-1)\theta+j}\right]^2, \tag{24}$$

$$\begin{aligned} C_1 = &\sum_{p=1}^{P}\sum_{j=1}^{\theta}\sum_{l=1}^{L} 2\alpha_l w_{R,p}^2 w_{I_u,p} x_{(p-1)\theta+j-\tau_l} n_{(p-1)\theta+j} \\ &+ \sum_{p=1}^{P}\sum_{j=1}^{\theta}\sum_{l=1}^{L} 2\alpha_l w_{R,p} w_{I_u,p} x_{(p-1)\theta+j-\tau_l} n_{(p-1)\theta+j} \\ &\times \sum_{i=1}^{U} \left(a_i w_{I_i,p} + b_i w_{Q_i,p}\right). \end{aligned} \tag{25}$$

Therefore, when $n = I_u$, the mean and variance of decision variable z_{I_u} can be calculated as

$$\begin{aligned} \mu_{I,1} &= \mathrm{E}\left[z_{I_u}\right] = \mathrm{E}[A_1] + \mathrm{E}[B_1] + \mathrm{E}[C_1] \\ &= \sum_{l=1}^{L} \alpha_l^2 2a_u P\theta \mathrm{E}\left[x_{(p-1)\theta+j-\tau_l}^2\right] = \sum_{l=1}^{L} \alpha_l^2 \frac{2a_u E_s}{1+U}, \end{aligned} \tag{26}$$

$$\begin{aligned} \sigma_{I,1}^2 &= \mathrm{Var}\left[z_{I_u}\right] = \mathrm{Var}[A_1] + \mathrm{Var}[B_1] + \mathrm{Var}[C_1] \\ &= \sum_{l=1}^{L} \alpha_l^2 4(1+U) P\theta \mathrm{E}\left[x_{(p-1)\theta+j-\tau_l}^2\right] \frac{N_0}{2} + P\theta \frac{N_0^2}{2} \\ &= 2\sum_{l=1}^{L} \alpha_l^2 E_s N_0 + \beta \frac{N_0^2}{2}, \end{aligned} \tag{27}$$

where E_s is the symbol energy of I/Q-CIM-CS-MDCSK, given as $E_s = (1+U)P\theta \mathrm{E}\left[x_{(p-1)\theta+j-\tau_l}^2\right]$.

Similarly, when the in-phase Walsh code detection is incorrect, namely $n = I_u' \neq I_u$, the component A_2 is obtained as follows: (see (28)) . In addition, the components B_2 and C_2 are given, respectively, as

$$B_2 = \sum_{p=1}^{P}\sum_{j=1}^{\theta} w_{R,p} w_{n,p} \left[n_{(p-1)\theta+j}\right]^2, \tag{29}$$

$$\begin{aligned} C_2 = &\sum_{p=1}^{P}\sum_{j=1}^{\theta}\sum_{l=1}^{L} 2\alpha_l w_{R,p}^2 w_{n,p} x_{(p-1)\theta+j-\tau_l} n_{(p-1)\theta+j} \\ &+ \sum_{p=1}^{P}\sum_{j=1}^{\theta}\sum_{l=1}^{L} 2\alpha_l w_{R,p} w_{n,p} x_{(p-1)\theta+j-\tau_l} n_{(p-1)\theta+j} \\ &\times \sum_{i=1}^{U} \left(a_i w_{I_i,p} + b_i w_{Q_i,p}\right). \end{aligned} \tag{30}$$

In this vein, when $n = \hat{I}_u \neq I_u$, the mean and variance of decision variable $z_{\hat{I}_u}$ can be easily calculated as

$$\mu_{I,2} = \mathrm{E}\left[z_{\hat{I}_u}\right] = 0, \tag{31}$$

$$\sigma_{I,2}^2 = \mathrm{Var}\left[z_{\hat{I}_u}\right] = 2\sum_{l=1}^{L} \alpha_l^2 E_s N_0 + \beta \frac{N_0^2}{2}. \tag{32}$$

$$\begin{aligned} z_{I_u} &= \sum_{p=1}^{P}\sum_{j=1}^{\theta} w_{R,p} w_{n,p} \left[\sum_{l=1}^{L} \alpha_l \left(w_{R,p} x_{(p-1)\theta+j-\tau_l} + \sum_{u=1}^{U} \left(a_u w_{I_u,p} + b_u w_{Q_u,p}\right) x_{(p-1)\theta+j-\tau_l}\right) + n_{(p-1)\theta+j}\right]^2 \\ &= \underbrace{\sum_{p=1}^{P}\sum_{j=1}^{\theta} w_{R,p} w_{n,p} \left[\sum_{l=1}^{L} \alpha_l \left(w_{R,p} + \sum_{u=1}^{U} \left(a_u w_{I_u,p} + b_u w_{Q_u,p}\right)\right) x_{(p-1)\theta+j-\tau_l}\right]^2}_{A} + \underbrace{\sum_{p=1}^{P}\sum_{j=1}^{\theta} w_{R,p} w_{n,p} \left[n_{(p-1)\theta+j}\right]^2}_{B} \\ &\quad + \underbrace{\sum_{p=1}^{P}\sum_{j=1}^{\theta} 2 w_{R,p} w_{n,p} \left[\sum_{l=1}^{L} \alpha_l \left(w_{R,p} + \sum_{u=1}^{U} \left(a_u w_{I_u,p} + b_u w_{Q_u,p}\right)\right) x_{(p-1)\theta+j-\tau_l}\right] n_{(p-1)\theta+j}}_{C}. \end{aligned} \tag{22}$$

$$\begin{aligned} A_1 = &\underbrace{\sum_{p=1}^{P}\sum_{j=1}^{\theta}\sum_{l=1}^{L} \alpha_l^2 w_{R,p} w_{I_u,p} w_{R,p}^2 x_{(p-1)\theta+j-\tau_l}^2}_{=0} + \underbrace{\sum_{p=1}^{P}\sum_{j=1}^{\theta}\sum_{i=1}^{U}\sum_{l=1}^{L} \alpha_l^2 a_i w_{R,p} w_{I_u,p} w_{I_i,p}^2 x_{(p-1)\theta+j-\tau_l}^2}_{=0} \\ &+ \underbrace{\sum_{p=1}^{P}\sum_{j=1}^{\theta}\sum_{i=1}^{U}\sum_{l=1}^{L} \alpha_l^2 b_i w_{R,p} w_{I_u,p} w_{Q_i,p}^2 x_{(p-1)\theta+j-\tau_l}^2}_{=0} + \underbrace{2\sum_{p=1}^{P}\sum_{j=1}^{\theta}\sum_{i=1}^{U}\sum_{l=1}^{L} \alpha_l^2 a_i b_i w_{R,p} w_{I_u,p} w_{I_i,p} w_{Q_i,p} x_{(p-1)\theta+j-\tau_l}^2}_{=0} \\ &+ \underbrace{2\sum_{p=1}^{P}\sum_{j=1}^{\theta}\sum_{i=1}^{U}\sum_{l=1}^{L} \alpha_l^2 b_i w_{R,p}^2 w_{I_u,p} w_{Q_i,p} x_{(p-1)\theta+j-\tau_l}^2}_{=0} + \underbrace{2\sum_{p=1}^{P}\sum_{j=1}^{\theta}\sum_{i=1,i\neq u}^{U}\sum_{l=1}^{L} \alpha_l^2 a_i w_{R,p}^2 w_{I_u,p} w_{I_i,p} x_{(p-1)\theta+j-\tau_l}^2}_{=0} \\ &+ 2\sum_{p=1}^{P}\sum_{j=1}^{\theta}\sum_{l=1}^{L} \alpha_l^2 a_u w_{R,p}^2 w_{I_u,p}^2 x_{(p-1)\theta+j-\tau_l}^2. \end{aligned} \tag{23}$$

$$
\begin{aligned}
A_2 = & \underbrace{\sum_{p=1}^{P}\sum_{j=1}^{\theta}\sum_{l=1}^{L}\alpha_l^2 w_{R,p} w_{n,p} w_{R,p}^2 x_{(p-1)\theta+j-\tau_l}^2}_{=0} + \underbrace{\sum_{p=1}^{P}\sum_{j=1}^{\theta}\sum_{i=1}^{U}\sum_{l=1}^{L}\alpha_l^2 a_i w_{R,p} w_{n,p} w_{I_i,p}^2 x_{(p-1)\theta+j-\tau_l}^2}_{=0} \\
& + \underbrace{\sum_{p=1}^{P}\sum_{j=1}^{\theta}\sum_{i=1}^{U}\sum_{l=1}^{L}\alpha_l^2 b_i w_{R,p} w_{n,p} w_{Q_i,p}^2 x_{(p-1)\theta+j-\tau_l}^2}_{=0} + \underbrace{2\sum_{p=1}^{P}\sum_{j=1}^{\theta}\sum_{i=1}^{U}\sum_{l=1}^{L}\alpha_l^2 a_i b_i w_{R,p} w_{n,p} w_{I_i,p} w_{Q_i,p} x_{(p-1)\theta+j-\tau_l}^2}_{=0} \\
& + \underbrace{2\sum_{p=1}^{P}\sum_{j=1}^{\theta}\sum_{i=1}^{U}\sum_{l=1}^{L}\alpha_l^2 b_i w_{R,p}^2 w_{n,p} w_{Q_i,p} x_{(p-1)\theta+j-\tau_l}^2}_{=0} + \underbrace{2\sum_{p=1}^{P}\sum_{j=1}^{\theta}\sum_{l=1}^{L}\alpha_l^2 a_u w_{R,p}^2 w_{n,p} w_{I_u,p} x_{(p-1)\theta+j-\tau_l}^2}_{=0} \\
& + \underbrace{2\sum_{p=1}^{P}\sum_{j=1}^{\theta}\sum_{i=1,i\neq u}^{U}\sum_{l=1}^{L}\alpha_l^2 a_i w_{R,p}^2 w_{n,p} w_{I_i,p} x_{(p-1)\theta+j-\tau_l}^2}_{=0}.
\end{aligned}
\tag{28}
$$